Application of TLM and Cassie-Mayr Arc model on Transformer Aging and Incipient Faults Simulation

X. Wang, M. Sumner and D. W. P. Thomas *

Abstract—**The development of the transformer insulation failure undergoes three stages: insulation aging, incipient faults and a short circuit. This paper presents a complete scheme to simulate single-phase transformers with insulation deterioration and arcing phenomena i.e. in the first two stages. The approach incorporates Transmission Line Methods (TLM), Jiles-Atherton Hysteretic Model, Composite Cassie-Mayr Arcing Model and Dielectric Model. A small 25kVA 11kV/220V power transformer with aging and incipient faults is taken as example for simulation.**

Keywords:* *Deterioration, Incipient Fault, Insulation Aging, Transformer, Transmission Line Methods (TLM)

1 Introduction

One of the most important electrical units in power system is transformer, the stability of which is significant for the reliability of the whole supply. Therefore various protection and monitoring schemes were developed in the last few decades. By now the differential relay that depends on the current difference to trigger the execution units is widely applied in the transformer protection against internal faults[1]. With the aspect of transformer monitoring, lots of practical experience is accumulated during the periodical preventative experiments, while the state-based maintenance and hence online monitoring are developing rapidly. Although can not directly reflect the remaining life of the transformer, dissolved gas and partial discharge are still the most common monitored items under the major circumstance. In fact each scheme can be regarded as a recognition procedure, the key issue of which is how to effectively distinguish the major faults arising within transformers.

A survey of the modern transformer breakdowns, which took place over a period of years, showed that 70%-80% of faults could be attributed to the failure of the internal insulation between winding turns[2]. As a result, such internal insulation faults inevitably become the main investigated subjects. Actually the development from a perfect condition to a complete breakdown undergoes several stages, which are insulation aging, incipient fault and a short circuit. After a transformer is installed on a site and because of some electrical, thermal or chemical effects, the internal insulation always weakens although it may develop very slowly. This deterioration is called aging, the main feature of which is the higher leakage current flowing through the insulation dielectric than the perfect condition. When the insulation degrades further, incipient faults appear in the form of some intermittent arcs within the insulation dielectric material. In such a case, if the transformer does not stop operating, the incipient faults will eventually turn into a permanent inter-turn short circuit that can cause serious damage and an outage. Since most faults mentioned above are destructive, it's desirable to undertake an accurate simulation to facilitate analysis and distinguish the characteristics of different stages in the deterioration of the insulation before the laboratory experiment.

D.J.Wilcox introduced a time-domain modal analysis which described how a transformer model could be converted from the frequency domain into the time domain for ATP/EMTP implementation[3], but it did not consider the existence of internal faults. For the transformer with internal faults, Patrick presented the matrix model that can be easily obtained by the calculation on the inductance of the healthy transformer, so that it can be simulated by EMTP[4]. But some idealized assumptions on which Patrick's model is based may affect its results. Hang Wang and Karen L. Butler proposed that the simulation results be acquired from the standpoint of electromagnetic fields with the assistance of finite element softwares e.g. ANSOFT's Maxwell[5]. The effects of insulation aging and incipient faults were exhibited by the parallel connection of a constant voltage source with an increasing resistance. The validity of this method was confirmed by experiments. However on the other hand, the application of more sophisticated Composite Cassie-Mayr theory in modelling arc has proved to be more successful[6][7].

*All authors are with George Green Institute for Electromagnetics Research, School of Electrical and Electronic Engineering, University of Nottingham, Nottingham, United Kingdom NG7 2RD. Email: xiaohui.wang@ieee.org. Manuscript was submitted on 05 September 2007

So following the authors' previous work on simulation of internal short circuit faults[8], a method, which incorporates Transmission Line Methods (TLM), Jiles-Atherton model for magnetic hysteresis and Composite Cassie-Mayr description of arc, is presented in this paper.

2 Transformer Model with Aging and Incipient Fault

A single-phase two-winding transformer impedance is represented by two matrices $[R]$ and $[L]$ as follows, where suffixes p and s are for the primary and the secondary respectively; R_i and L_{ii} are the resistance and the self inductance of winding i; M_{ij} is the mutual inductance between winding i and j.

$$[R] = \begin{bmatrix} R_p & 0 \\ 0 & R_s \end{bmatrix} \quad [L] = \begin{bmatrix} L_{pp} & M_{ps} \\ M_{sp} & L_{ss} \end{bmatrix} \tag{1}$$

The terminal voltages and currents are then related by

$$\begin{bmatrix} u_p \\ u_s \end{bmatrix} = [R] \begin{bmatrix} i_p \\ i_s \end{bmatrix} + [L] \frac{d \begin{bmatrix} i_p \\ i_s \end{bmatrix}}{dt} \tag{2}$$

where u_i is the voltage and i_i is the current of winding i.

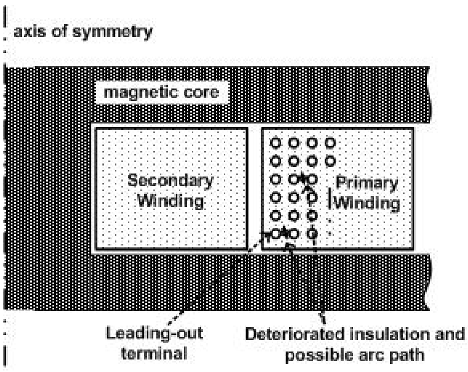

Figure 1: Diagram of deteriorated insulation and possible arcing path

After the transformer operates for a period, the insulation within the protection zone inevitably deteriorates. For a shell type transformer, the weakest insulation is usually at the locations between two adjacent layers of the winding. So the effects of aging can be severe at these points. For example, the severest deterioration may take place in the primary as shown in Figure.1 (marked points). And from the fault location, the primary winding may be divided to two (Figure.2(a)) or three sub-windings (Figure.2(b)).

Accordingly the matrices $[R]$ and $[L]$ in the expression (1) are converted to the matrices in the expression (3) for the configuration in Figure.2(a) and those in the expression (5) for the configuration in Figure.2(b)

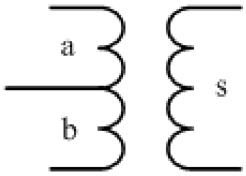

(a) Deterioration between leading-out terminal and adjacent layer

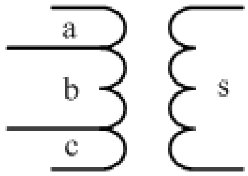

(b) Deterioration between two internal adjacent layers

Figure 2: Diagram of sub-windings in transformer with insulation deterioration in the primary

$$[R] = \begin{bmatrix} R_a & 0 & 0 \\ 0 & R_b & 0 \\ 0 & 0 & R_s \end{bmatrix} \quad [L] = \begin{bmatrix} L_{aa} & M_{ab} & M_{as} \\ M_{ba} & L_{bb} & M_{bs} \\ M_{sa} & M_{sb} & L_{ss} \end{bmatrix} \tag{3}$$

$$\begin{bmatrix} u_a \\ u_b \\ u_s \end{bmatrix} = [R] \begin{bmatrix} i_a \\ i_b \\ i_s \end{bmatrix} + [L] \frac{d \begin{bmatrix} i_a \\ i_b \\ i_s \end{bmatrix}}{dt} \tag{4}$$

$$[R] = \begin{bmatrix} R_a & 0 & 0 & 0 \\ 0 & R_b & 0 & 0 \\ 0 & 0 & R_c & 0 \\ 0 & 0 & 0 & R_s \end{bmatrix}$$

$$[L] = \begin{bmatrix} L_{aa} & M_{ab} & M_{ac} & M_{as} \\ M_{ba} & L_{bb} & M_{bc} & M_{bs} \\ M_{ca} & M_{cb} & L_{cc} & M_{cs} \\ M_{sa} & M_{sb} & M_{sc} & L_{ss} \end{bmatrix} \tag{5}$$

$$\begin{bmatrix} u_a \\ u_b \\ u_c \\ u_s \end{bmatrix} = [R] \begin{bmatrix} i_a \\ i_b \\ i_c \\ i_s \end{bmatrix} + [L] \frac{d \begin{bmatrix} i_a \\ i_b \\ i_c \\ i_s \end{bmatrix}}{dt} \tag{6}$$

2.1 Aging Model

Traditionally the low frequency behavior of dielectric material can be represented in terms of an equivalent parallel circuit as shown in Figure.3, where u_d, i_d, R_d and C_d are applied voltage, leakage current through dielectric, insulation resistance and parasite capacitance respectively. According to the literature[5] and experimental results, the equivalent capacitance C_d changes little during the deterioration of insulation. Resistance R_d is large in the case of perfect insulation, while it decreases significantly with the effect of aging.

For considering the aging condition of the dielectric, the equivalent circuit in Figure.2 becomes as given in Figure.4. And the additional expression is generated ($u_d = u_b$).

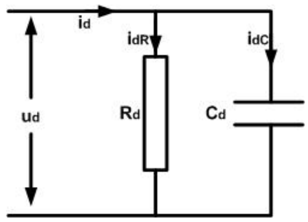

Figure 3: Equivalent circuit of insulation dielectric

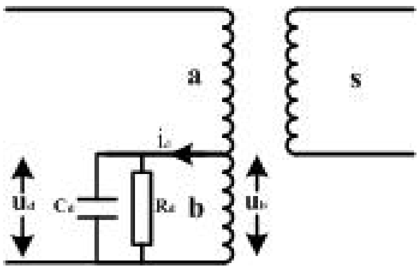

(a) Deterioration between leading-out terminal and adjacent layer

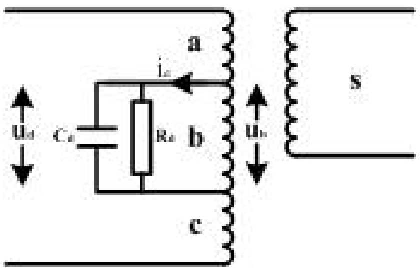

(b) Deterioration between two internal adjacent layers

Figure 4: Diagram of transformer with aging model in the primary

$$i_d = i_a - i_b = \frac{1}{R_d} u_b + C_d \frac{du_b}{dt} \tag{7}$$

2.2 Arc Model

When the insulation degrades further, some intermittent arcs i.e. incipient faults begin to persist within the insulation. The process of arcing can be divided into extinction stage and recovery stage. The former one lasts a few microseconds from the beginning of the arcing to the moment when the arc current reaches zero, while the latter one follows in time.

As two special cases of black box arc models, Cassie and Mayr arc model have the general forms[9] given in the equations (8):

$$\frac{du}{dt} = \Phi(u,i)\frac{di}{dt} - uF(u,i)$$

$$\Phi(u,i) = \frac{u}{i}$$

$$F_M(u,i) = \frac{1}{\theta}\left(\frac{ui}{N_0} - 1\right) for Mayr Model$$

$$F_C(u,i) = \frac{1}{\theta}\left(\frac{u^2}{E_0} - 1\right) for Cassie Model \tag{8}$$

where θ represents the arc time constant, u and i are the arc voltage and current respectively.

Then the composite Cassie-Mayr method models arcing phenomena by modifying the value of the arc resistance i.e. insulation resistance R_d in Figure.4. When the voltage over the resistance R_d is larger than the constant arc voltage E_0 in case of steady state, the extinction stage begins. During this stage, the resistance is dominated by the Cassie's equation with the initial value of R_d being the one in the aging model:

$$\frac{1}{R_d}\frac{dR_d}{dt} = \frac{1}{\theta}\left(1 - \frac{u_d^2}{E_0^2}\right) \tag{9}$$

After the current i_{dR} decreases to zero, the arc is completely extinguished. Then the recovery stage begins which can be represented by the Mayr's equation.

$$\frac{1}{R_d}\frac{dR_d}{dt} = \frac{1}{\theta}\left(1 - \frac{u_d i_{R_d}}{N_0}\right) \tag{10}$$

Where $N_0 = E_0 I\omega\theta$, I is the rms value of the interrupted current in ampere. If the arc resistance R_d computed by Mayr's equation starts to decrease, indicating reignition, Cassie's differential equation (9) is used with a new value $E_0 = \sqrt{N_0 R_m}$ from the point the arc resistance has reached the maximum value R_m. If the arc resistance R_d keeps increasing until it reaches the value before arc starts, then the entire arcing process ends. And after this point, the aging model returns for use.

2.3 Hysteresis Model

For modelling nonlinear hysteretic cores the approach applied here is to use the Jiles-Atherton model (J-A model) [10] to introduce hysteretic behavior. Based on the constitutive relationship for the flux density $B = \mu_0(H+M)$, where μ_0 is the permeability of free space, H is the magnetic flux density and M is the magnetising intensity, each inductance in the matrices (3) and (5) are decomposed.

Equations (4) and (6) including non-linear inductance are given in equations (11) and (12) respectively.

$$\begin{bmatrix} u_a \\ u_b \\ u_s \end{bmatrix} = \begin{bmatrix} R_a & 0 & 0 \\ 0 & R_b & 0 \\ 0 & 0 & R_s \end{bmatrix} \begin{bmatrix} i_a \\ i_b \\ i_s \end{bmatrix} + \begin{bmatrix} L'_{aa} & M'_{ab} & M'_{as} & N_a L_m \\ M'_{ba} & L'_{bb} & M'_{bs} & N_b L_m \\ M'_{sa} & M'_{sb} & L'_{ss} & N_s L_m \end{bmatrix} \frac{d\begin{bmatrix} i_a \\ i_b \\ i_s \\ i_m \end{bmatrix}}{dt} \tag{11}$$

$$\begin{bmatrix} u_a \\ u_b \\ u_c \\ u_s \end{bmatrix} = \begin{bmatrix} R_a & 0 & 0 & 0 \\ 0 & R_b & 0 & 0 \\ 0 & 0 & R_c & 0 \\ 0 & 0 & 0 & R_s \end{bmatrix} \begin{bmatrix} i_a \\ i_b \\ i_c \\ i_s \end{bmatrix}$$

$$+ \begin{bmatrix} L'_{aa} & M'_{ab} & M'_{ac} & M'_{as} & N_a L_m \\ M'_{ba} & L'_{bb} & M'_{bc} & M'_{bs} & N_b L_m \\ M'_{ca} & M'_{cb} & L'_{cc} & M'_{cs} & N_c L_m \\ M'_{sa} & M'_{sb} & M'_{sc} & L'_{ss} & N_s L_m \end{bmatrix} \frac{d \begin{bmatrix} i_a \\ i_b \\ i_c \\ i_s \\ i_m \end{bmatrix}}{dt} \tag{12}$$

where i_m is the normalized magnetization given by $i_m = Ml$ and L'_{ii}/M'_{ij} are self/mutual inductance in the situation where the transformer core is removed and replaced by air. L'_{ii}/M'_{ij} and L_m can either be deduced from the expressions for impedances given by Wilcox et. al [11][12] or approximated by

$$M'_{ij} = \frac{\mu_0 N_i N_j A}{l} \tag{13}$$

$$L_m = \frac{\mu_0 A}{l} \tag{14}$$

The classical J-A model [10][13] is described in the following subsections:

2.3.1 Weighting coefficient

The magnetization is split into two parts, the anhysteretic magnetization and the irreversible magnetization. In normalized form, this is expressed by

$$i_m = \beta_c i_{an} + (1 - \beta_c) i_{irr} \tag{15}$$

where β_c is the weighting coefficient with $0 \le \beta_c \le 1$, i_{an} is the normalized anhysteretic magnetization and i_{irr} is the normalized irreversible magnetization.

2.3.2 Modified langevin function

The anhysteretic magnetization dependence is given by a modified Langevin function, i.e.

$$i_{an} = i_{sat} \left[coth \left(\frac{i_L + \alpha i_m}{i_{aht}} \right) - \frac{i_{aht}}{i_L + \alpha i_m} \right] = i_{sat} L(\gamma) \tag{16}$$

where i_L is the ampere-turn sum of all exciting currents, i_{sat} is the normalized saturation magnetization, α is the interdomain coupling coefficient and i_{aht} is the normalized anhysteretic magnetization form factor. The coefficients i_{sat}, α, i_{aht} are positive constants. Also $L(\gamma)$ denotes the modified Langevin function with argument $\gamma = \frac{i_L + \alpha i_m}{i_{aht}}$. To avoid difficulties with the modified Langevin function for small arguments, a linear approximation is used where for $|\gamma| < 0.001$ we put $L(\gamma) \approx \frac{\gamma}{3}$.

2.3.3 Differential equation for the irreversible magnetization

In the Jiles-Atherton model, the derivative of the normalized irreversible magnetization with respect to the inductor current is

$$\frac{di_{irr}}{di_L} = \left[\frac{\delta_m (i_{an} - i_{irr})}{\delta i_{coe} - \alpha (i_{an} - i_{irr})} \right] \tag{17}$$

where the migration flag δ_m is given by:

$$\delta_m = \begin{cases} 1 & : \ if \ \frac{di_L}{dt} > 0 \ and \ i_{an} > i_{irr} \\ 1 & : \ if \ \frac{di_L}{dt} < 0 \ and \ i_{an} < i_{irr} \\ 0 & : \ otherwise \end{cases} \tag{18}$$

3 TLM Modelling

The transformer equations are solved using the time domain TLM method as described in [14]. In TLM an inductor element is represented by a short circuited transmission line stub as given in Figure. 5, which is reduced to a serial voltage source and surge impedance as shown. At each time step n the following equations are solved.

$$u_n = Z_L i_n + 2u_n^i \tag{19}$$

$$u_n = u_n^i + u_n^r \tag{20}$$

$$u_{n+1}^i = -u_n^r \tag{21}$$

where $Z_L = \frac{2L}{\Delta t}$; Δt is the time length of each step; the suffix n stands for the nth time step; u_n^i is the incident voltage in nth time step; u_n^r is the reflected voltage in nth time step.

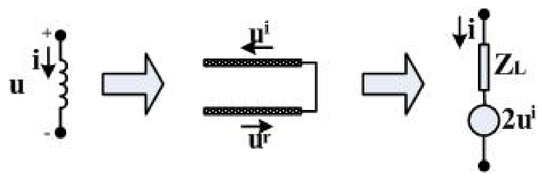

Figure 5: Representation of Inductor in TLM

Similarly a capacitor element can be described by an open circuited transmission line stub as given in Figure.6 and the iterative equations are

$$u_n = Z_C i_n + 2u_n^i \tag{22}$$

$$u_n = u_n^i + u_n^r \tag{23}$$

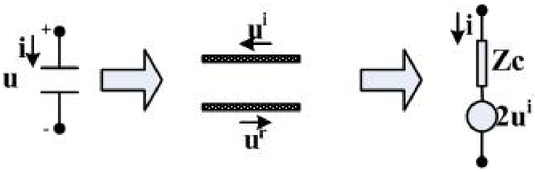

Figure 6: Representation of Capacitor in TLM

$$u^i_{n+1} = u^r_n \quad (24)$$

where $Z_C = \frac{\Delta t}{2C}$

Therefore for the simulation of an aging or arcing transformer with a nonlinear hysteretic core and with the terminal relationships as turn to earth fault as given by equation (11) and Figure.4(a): the self impedances (inductances) can be modelled as given by equations (25), the controlled sources representing mutual terms of the type $M'_{ij}\frac{di_j}{dt}$ are given by equation (26) and the capacitor C_d is represented by equation (27) as follows:

$$u_{ii} = Z_{ii}i_i + 2u^i_{ii} \quad (25)$$

$$u_{ij} = Z_{ij}i_j + 2u^i_{ij} \quad (26)$$

$$u_d = Z_d i_{dc} + 2u^i_d \quad (27)$$

where $Z_{ii} = \frac{2L'_{ii}}{\Delta t}$; $Z_{ij} = \frac{2M'_{ij}}{\Delta t}$; $Z_d = \frac{\Delta t}{2C_d}$ and there is a term representing the magnetization $L_m\frac{di_m}{dt}$ given by

$$u_m = Z_m i_m + 2u^i_m \quad (28)$$

where $Z_m = \frac{2L_m}{\Delta t}$

The magnetization i_m is non-linear so that an iterative solution for the following simultaneous equations has to be found.

$$\begin{aligned} f_1 &= (Z_{aa}+R_a)i_a + Z_{ab}i_b + Z_{as}i_s \\ &+(Z_d \parallel R_d)(i_a - i_b) + N_a Z_m i_m - u_{src} \\ &+2(u^i_{aa} + u^i_{ab} + u^i_{as} + \frac{u^i_d R_d}{R_d + Z_d} + N_a u^i_m) = 0 \end{aligned} \quad (29)$$

$$\begin{aligned} f_2 &= Z_{ba}i_a + Z_{bb}i_b + Z_{bs}i_s \\ &-(Z_d \parallel R_d)(i_a - i_b) + N_b Z_m i_m \\ &+2(u^i_{ba} + u^i_{bb} + u^i_{bs} - \frac{u^i_d R_d}{R_d + Z_d} + N_b u^i_m) = 0 \end{aligned} \quad (30)$$

$$\begin{aligned} f_3 &= Z_{sa}i_a + Z_{sb}i_b + (Z_{ss} + R_s + Z_{load} + R_{load})i_s \\ &+N_s Z_m i_m + 2(u^i_{sa} + u^i_{sb} + u^i_{ss} + u^i_{load} + N_s u^i_m) = 0 \end{aligned} \quad (31)$$

We have chosen the Newton-Raphson technique for its efficiency and stability so the solution is found through the following iterative procedure

$$\begin{bmatrix} i_a \\ i_b \\ i_s \end{bmatrix}_{p+1} = \begin{bmatrix} i_a \\ i_b \\ i_s \end{bmatrix}_p - \begin{bmatrix} \frac{\partial f_1}{\partial I_a} & \frac{\partial f_1}{\partial I_b} & \frac{\partial f_1}{\partial I_s} \\ \frac{\partial f_2}{\partial I_a} & \frac{\partial f_2}{\partial I_b} & \frac{\partial f_2}{\partial I_s} \\ \frac{\partial f_3}{\partial I_a} & \frac{\partial f_3}{\partial I_b} & \frac{\partial f_3}{\partial I_s} \end{bmatrix}^{-1}_p \begin{bmatrix} f_1 \\ f_2 \\ f_3 \end{bmatrix}_p \quad (32)$$

where p is the iteration number and

The iteration is started with initial values taken from the TLM previous time step and continued until suitable convergence criteria are met. In this work this is set as

$$\left|(i_a)_{p+1} - (i_a)_p\right| < \tau \text{ and } \left|(i_b)_{p+1} - (i_b)_p\right| < \tau$$
$$\text{and } \left|(i_s)_{p+1} - (i_s)_p\right| < \tau$$

Similarly for the simulation of transformer with turn to turn fault governed by equation (12) and Figure.4(b)

$$\begin{aligned} f_1 &= (Z_{aa} + Z_{ac} + R_a + Z_{ca} + Z_{cc} + R_c)i_a \\ &+(Z_{ab} + Z_{cb})i_b + (Z_{as} + Z_{cs})i_s \\ &+(Z_d \parallel R_d)(i_a - i_b) + (N_a + N_c)Z_m i_m \\ &-u_{src} + 2(u^i_{aa} + u^i_{ab} + u^i_{ac} + u^i_{as} + u^i_{ca} + u^i_{cb} \\ &+u^i_{cc} + u^i_{cs} + \frac{u^i_d R_d}{R_d + Z_d} + (N_a + N_c)u^i_m) = 0 \end{aligned} \quad (33)$$

$$\begin{aligned} f_2 &= (Z_{ba} + Z_{bc})i_a + Z_{bb}i_b + Z_{bs}i_s \\ &-(Z_d \parallel R_d)(i_a - i_b) + N_b Z_m i_m \\ &+2(u^i_{ba} + u^i_{bb} + u^i_{bc} + u^i_{bs} - \frac{u^i_d R_d}{R_d + Z_d} + N_b u^i_m) = 0 \end{aligned} \quad (34)$$

$$\begin{aligned} f_3 &= (Z_{sa} + Z_{sc})i_a + Z_{sb}i_b \\ &+(Z_{ss} + R_s + Z_{load} + R_{load})i_s + N_s Z_m i_m \\ &+2(u^i_{sa} + u^i_{sb} + u^i_{sc} + u^i_{ss} + u^i_{load} + N_s u^i_m) = 0 \end{aligned} \quad (35)$$

Note that $i_a = i_c$ and hence only i_a is required to be solved

4 Simulation Results

A small 25kVA, 11kV/220V power transformer with the geometry given in Fig. 7 is modelled so as to demonstrate the modelling procedure. The Jiles-Atherton parameters are typical of a core made of FeSi sheets [15].

Figure.8 and Figure.9 show some simulation results of the transformer with deterioration insulation in the primary winding. Parameters of the aging model and Cassie-Mayr arc model are as follows: $R_d = 1400\Omega$;$C_d = 6.06pF$;$E_0 = 397.22V$;$\theta = 0.1ms$. During the time section from $0.5s$ to $0.55s$, three arcs take place and some characteristics of arcs can be observed e.g. the arc voltage is almost a flat-top waveform as shown in Figure.8(d) and Figure.9(c).

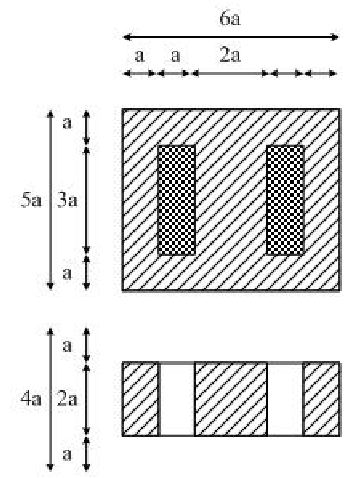

Figure 7: 25kVA 11kV/220V power transformer geometry. Unit $a = 0.0587375m$ and magnetic path length $l = 12a$. Number of turns in primary $N_p = 2509$; Number of turns in secondary $N_s = 51$. Jiles-Atherton parameters: Saturation magnetization $M_s = 1.47 \times 10^6 A/m$; Anhysteretic form factor $H_a = 40.0A/m$; Interdomain coupling coefficient $\alpha = 0.00008$; Coercive field magnitude $H_c = 60.0A/m$; Magnetization weighting factor β_c=0.55; Supply voltage source: resistance $R_{src} = 1.565\Omega$, inductance $L_{src} = 2.4132\mu H$

5 Conclusion and Future Work

By incorporating Transmission Line Methods (TLM), Jiles-Atherton Hysteretic Model, Composite Cassie-Mayr Arcing Model and Dielectric Model, the simulation results of transformer with aging insulation and incipient faults can be acquired. Although the results seem reasonable, they need to be validated by the experiments.

References

[1] A. C. Franklin and D. P. Franklin, *The J&P Transformer Book 11th Edition*, England: Butterworth & Co. (Publishers) Ltd., 1983.

[2] K. L. Butler and M. Bagriyanik, ”Identifying transformer incipient events for maintaining distribution system reliability,” in *Proceedings of the 36th Hawaii International Conference on System Sciences*, 2003.

[3] D. J. Wilcox, M. Conlon, D. J. Leonard and T. P. McHale, ”Time-domain modelling of power transformers using modal analysis,” *IEE Proceeding: Electric Power Application*, vol. 144, no. 2, pp. 77-83, March 1997.

[4] P. Bastard, P. Bertrand and M. Mevnier, ”A Transformer model for winding fault studies,” *IEEE Trans. on Power Delivery*, vol. 9, no. 2, April 1994.

[5] H. Wang and K. L. Butler, ”Modeling transformers with internal incipient faults,” *IEEE Trans. on Power Delivery*, vol. 17, pp. 500-509, April 2002.

[6] D. W. P. Thomas, E. T. Pereira, C. Christopoulos and A. F. Howe, ”The simulation of circuit breaker switching using a composite cassie-modified mayr model,” *IEEE Trans. on Power Delivery*, vol. 10, no. 4, pp. 1829-1835, October 1995.

[7] S. Porkar, G. B. Gharehpetian, K. Feser, ”A disk-to-disk breakdown and arc modeling method for fault diagnosis of power transformers during impulse testing,” *Springer: Electrical Engineering*, vol. 86, pp. 261-265, 2004.

[8] X. Wang, M. Sumner and D. W. P. Thomas, ”Simulation of single-phase nonlinear and hysteretic transformer with internal faults,” in *Proceedings of Power Systems Conference and Exposition, PSCE’06. 2006 IEEE PES*, pp. 1075-1080, Atlanta, USA, October 2006.

[9] J. L. Guardado, S. G. Maximov, E. Melgoza, J. L. Naredo and P. Moreno, ”An improved arc model before current zero based on the combined Mayr and Cassie arc models,” *IEEE Trans. on Power Delivery*, vol. 20, no. 1, pp. 138-142, January 2005.

[10] D. C. Jiles, J. B. Thoelke and M. K. Devine, ”Numerical Determination of Hysteresis Parameters for the Modeling of Magnetic Properties Using the Theory of Ferromagnetic Hysteresis,” *IEEE Trans. on Magnetics*, vol. 28, no. 1, pp. 27-35, January 1992.

[11] D. J. Wilcox, M. Conlon and W. G. Hurley, ”Calculation of self and mutual impedances for coils on ferromagnetic cores,” *IEE Proceedings, Part A: Physical Science, Measurement and Instrumentation, Management and Education, Reviews*, vol. 135-A, no. 7, pp. 470-476, September 1988.

[12] D. J. Wilcox, W. G. Hurley and M. Conlon, ”Calculation of self and mutual impedances between sections of transformer windings,” *IEE Proceedings, Part C: Generation, Transmission and Distribution*, vol. 136, no. 5, pp. 308-314, September 1989.

[13] J. Paul, C. Christopoulos and D. W. P. Thomas, ”Time-domain simulation of nonlinear inductors displaying hysteresis,” *COMPUMAG 2003*, pp. 182-183, Saratoga Springs, New York, July 2003.

[14] C. Christopoulos, *The transmission-line modeling method : TLM*, New Jersey, USA: IEEE Press, 1995.

[15] A. Benabou, S. Clenet and F. Piriou, ”Comparison of Preisach and Jiles-Atherton models to take into account of hysteresis phenomenon for finite element analysis,” *Journal of magnetism and magnetic materials*, vol. 261, no. 1, pp. 139-160, 2003.

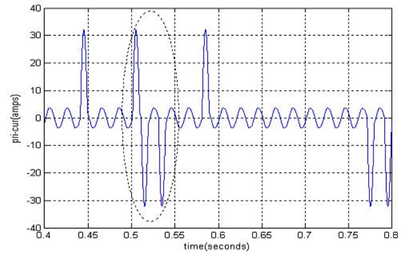

(a)

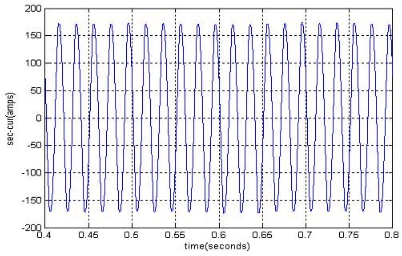

(b)

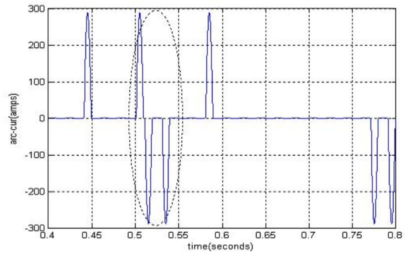

(c)

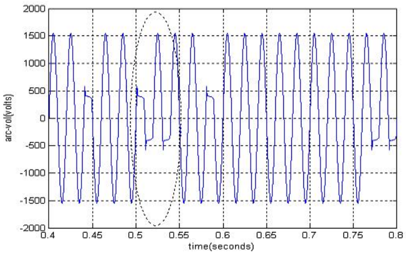

(d)

Figure 8: Terminal currents and arc voltage/current for the transformer with deterioration/aging insulation and some incipient faults between 125th and 375th turns on the primary winding. (a) Primary Current. (b) Secondary Current. (c) Arc Current. (d) Arc Voltage.

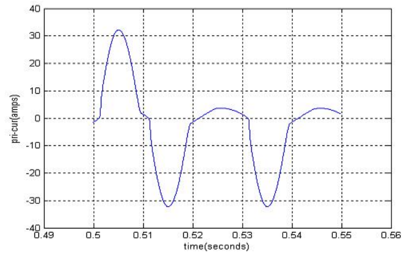

(a)

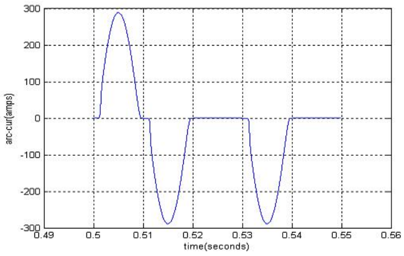

(b)

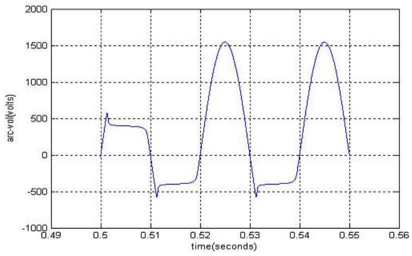

(c)

Figure 9: Zoomed in details of Figure.8 in dot circle (a) Primary Current. (b) Arc Current. (c) Arc Voltage.